Proceedings of The Internal Combustion Engine Fall Conference
ICEF 2021
October 13-15, 2021, Virtual , Online

ICEF2021- 67598

HIGH-FIDELITY ENERGY DEPOSITION IGNITION MODEL COUPLED WITH FLAME PROPAGATION MODELS AT ENGINE-LIKE FLOW CONDITIONS

Samuel J. Kazmouz
Energy Systems Division
Argonne National Laboratory
Lemont, IL 60439
Email: skazmouz@anl.gov

Riccardo Scarcelli
Energy Systems Division
Argonne National Laboratory
Lemont, IL 60439

Joohan Kim
Energy Systems Division
Argonne National Laboratory
Lemont, IL 60439

Zhen Cheng
Convergent Science, Inc.
Madison, WI 53719

Shuaishuai Liu
Convergent Science, Inc.
Madison, WI 53719

Meizhong Dai
Convergent Science, Inc.
Madison, WI 53719

Eric Pomraning
Convergent Science, Inc.
Madison, WI 53719

Peter K. Senecal
Convergent Science, Inc.
Madison, WI 53719

Seong-Young Lee
Michigan Technological University
Houghton, MI 49931

ABSTRACT

With the heightened pressure on car manufacturers to increase the efficiency and reduce the carbon emissions of their fleets, more challenging engine operation has become a viable option. Highly dilute, boosted, and stratified charge, among others, promise engine efficiency gains and emissions reductions. At such demanding engine conditions, the spark-ignition process is a key factor for the flame initiation propagation and the combustion event. From a computational standpoint, there exists multiple spark-ignition models that perform well under conventional conditions but are not truly predictive under strenuous engine operation modes, where the underlying physics needs to be expanded. In this paper, a hybrid Lagrangian-Eulerian spark-ignition (LESI) model is coupled with different turbulence models, grid sizes, and combustion models. The ignition model, previously developed, relies on coupling Eulerian energy deposition with a Lagrangian particle evolution of the spark channel, at every time-step. The spark channel is attached to the electrodes and allowed to elongate at a speed derived from the flow velocity. The LESI model is used to simulate spark ignition in a non-quiescent crossflow environment at engine-like conditions, using CONVERGE commercial CFD solver. The results highlight the consistency, robustness, and versatility of the model in a range of engine-like setups, from typical with RANS and a larger grid size to high fidelity with LES and a finer grid size. The flame kernel growth is then evaluated against schlieren images from an optical constant volume ignition chamber with a focus on the performance of flame propagation models, such as G-equation and thickened flame model, versus the baseline well-stirred reactor model. Finally, future development details are discussed.

INTRODUCTION

Light-duty vehicles (LDVs) are the most common form of transportation in the United States and, collectively, are responsible for the most energy consumption and greenhouse emissions in the sector [1]. Owing to several factors, among which are low production and maintenance costs, gasoline-powered spark ignition (SI) reciprocating internal combustion

engines are the most used technology in light duty vehicles [1]. As a result, efficiency improvements in SI engines would amplify to significant emission reductions on a national and global scale.

Automakers are at the forefront of innovation to increase engine efficiency and reduce their fleet emissions, through advanced and unconventional engine operation modes, such as highly dilute, boosted, and stratified-charge [2]. In addition, despite electric LDVs posing a challenge to the future of gasoline engines, the U.S. Energy Information Administration (EIA), in its 2021 energy outlook report, predicts that SI engines will remain a large part of the market by 2050 [1]. The ignition event in an SI engine is critical for engine stability, full burn cycles, and reduction in cyclic variability. Given its importance to flame initiation and sustained turbulent flame propagation, especially in unconventional engine operation, reliable and accurate spark ignition models are necessary to design ignition systems that reduce cyclic variability [3].

Computational spark ignition models have become synonymous with spark energy deposition and early flame formation. The transition from laminar flame kernel to turbulent flame also falls under ignition modeling [4, 5]. Typically, the ignition process starts with temporal and spatial plasma energy deposition, followed by kernel formation, and finally kernel to flame transition. However, the ignition modeling process cannot be described without the combustion model, as there is significant overlap and the coupling procedure depends on the chosen models.

In general, ignition models can be split between Eulerian [6–8] and Lagrangian [9–11]. The Eulerian approach usually (but not exclusively) relies on depositing a heat source on a refined finite volume Eulerian grid and allowing the pressure and temperature to expand and convect with the flow field (i.e. grid resolved). Eulerian approaches evolved from limited electrode geometries with a single energy source [6] to full engine geometries with multiple energy sources to represent the different stages of spark ignition [8]. The energy source could be a sphere (industry standard), cylinder, or even a line. Eulerian ignition models can also account for gas ionization. Eulerian approaches were limited in the past but gained more validity as computational power increased and attainable grid sizes decreased. Eulerian energy deposition models are more suited for finite-rate (or detailed) chemistry models such as the well-stirred reactor (WSR) and the thickened flame model (TFM). The coupling between the two is generally achieved by the temperature rise, which increases the Arrhenius source term in the species transport equation and subsequently reactant consumption. The ignition model generates a temperature rise through an energy source equivalent to the ignition energy generated by experiment (usually on the order of mJ and deposited in an L-shape profile to account for the different phases of the ignition process). The flame then sustains itself through species and heat diffusion. Fine grids are required because the early flame-flow interaction depends on the resolved velocity field and turbulence model. In addition, Eulerian models can be used with the G-equation model (industry standard) through a temperature cutoff criteria or g sourcing. In the temperature cutoff approach, G is initialized at temperatures higher than a set value (for example 3000 K), and propagates according to a turbulent flame expression. The value of the cutoff temperature can be tuned to improve flame initialization and formation. However, the early flame growth could be overestimated since immediate turbulent kernel behavior is assumed and the laminar to turbulent flame transition can be improved [5]. The T-cut approach overlooks turbulence/flame interactions and generates a flame kernel that bypasses flame growth physics, and thus leads to faster early flame propagation.

On the other hand, Lagrangian models, which have been the common type of ignition models in the past, rely on tracking points or kernels in space using turbulent or laminar flame speed correlations and solving transport properties to determine the size of the kernel. When the flame kernel reaches a critical size, the model switches to an Eulerian combustion model, typically a flamelet model. In general, Lagrangian models are designed to work with a specific turbulent combustion model [4, 12]. Most well known Lagrangian ignition models are DPIK [13], AKTIM [10], and SparkCIMM [12], which share a Lagrangian methodology to track the plasma channel using flame speed expressions, and initiate a flame kernel when certain criteria are met (such as Karlovitz number).

Both Lagrangian and Eulerian models can have additional sub-models, such as an on-board secondary circuit, short-circuit, blow-off, and re-strike [14–16]. With increased computational power, there has been a shift to the Eulerian approach and even historically Lagrangian ignition models have adopted a Eulerian formulation (for example AKTIM-Euler).

Inspired by the Lagrangian and Eulerian approaches, this paper presents results from ongoing work using a high fidelity energy deposition Lagrangian-Eulerian Spark Ignition (LESI) model. Development of spark ignition models at Argonne National Laboratory started with a detailed energy deposition study that established accurate source geometry, conjugate heat transfer, and detailed chemistry in a quiescent condition. It was concluded that with the correct input parameters, the model could predict the transition between ignition success and misfire at critical conditions [17]. LESI was then developed to model the glow phase of ignition in cross-flow (non-quiesent) conditions. The pre-glow (or breakdown) phase was modeled using offline equilibrium calculations to initialize pressure and temperature and account for species ionization.

In this paper, LESI is coupled with Arrhenius detailed chemistry based combustion models (WSR and TFM) and flamelet based combustion models (G-equation) to model spark channel elongation and kernel and flame development in a simplified constant volume combustion vessel at cross-flow

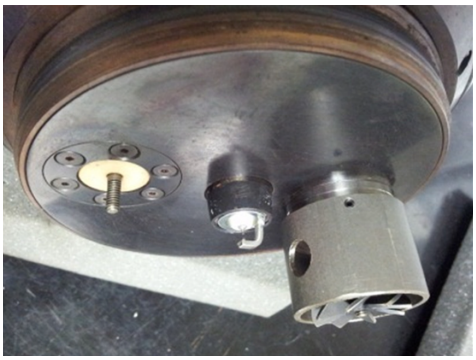

FIGURE 1. Interior of Combustion Vessel with Shrouded Fan to Generate Flow across the Spark Plug Gap

engine-like conditions using CONVERGE CFD solver [18]. First, an overview of the method is provided, including the experimental and computational setups. Then, the results using different turbulent combustion models are shown and the spark channel elongation and flame development are compared to experimental Schlieren images to assess the performance of different models.

EXPERIMENTAL SETUP

The results presented in this paper are validated against experiments carried out in a combustion vessel in the Alternative Fuels Combustion Laboratory (AFCL) at Michigan Technological University (MTU). The vessel has a total volume of 1.1 L and is equipped with 6 windows which can be used for mounting components such as spark plugs or for optical access to record data such as Schlieren or particle image velocimetry (PIV) data. The vessel body can be maintained at a constant temperature of up to 453 K, while the vessel can be operated up to a temperature of 2100 K and a pressure of 345 bar. The results presented in this paper are a continuation of previous validation work on LESI [19], which relied on both Schlieren and PIV data [20].

The vessel contains a shrouded fan designed to generate flow directed towards the spark plug, as shown in Fig. 1. The fan has eight straight blades (30 degree angle of attack) and a 25.4 mm outer diameter. The fan is powered by a 12 V DC motor, which is equipped with a control system that maintains the fan speed regardless of variations in pressure inside the vessel.

For this paper, the fan is set to 6000 rpm, which results in a velocity magnitude of around 2 m/s in the spark plug gap. During the PIV test, the spark plug was replaced with a solid adapter. Hence, the actual velocity with the spark plug installed might be slightly different than 2 m/s. A premixed mixture of Propane-EGR is allowed into the vessel and ignited by the spark plug mounted on the roof of the vessel (Fig. 1). The ignition and eventual flame growth are captured using a Schlieren technique.

TABLE 1. Details of Experimental Setup

Initial Pressure	16 bar
Initial Temperature	453 K
Fuel	Propane (C_3H_8)
Equivalence Ratio (ϕ)	0.9
EGR (by mass)	20%
Spark Plug Gap	0.9 mm
Spark Energy (Glow Phase)	30 mJ
Fan Speed	6000 rpm
Gap Velocity	2 m/s

The overall equivalence ratio is 0.9 and an EGR level of 20% by mass. The vessel is kept initially at a constant temperature of 453 K and an initial pressure of 16 bar. The secondary circuit current and voltage are recorded and used to calculate the total energy deposited during the glow phase of ignition. Details of the experimental case are shown in Table 1.

NUMERICAL SETUP

The computational domain is taken as a small section surrounding the spark plug near the top of the combustion vessel. As shown in Fig. 2, the domain includes inflow and outflow boundaries to mimic the flow originating from the shrouded fan. The spark plug, spark plug adapter, and portion of the top of the combustion vessel are treated as "solid-fluid interface", which is necessary to enable conjugate heat transfer (CHT) calculations. In addition, a solid slab of stainless steel (same material as the physical vessel) is added on top of the computational domain and set as the solid region. CHT is required for accurate calculations of heat loss to the walls during ignition. The rest of the boundaries are treated as walls. Similar to experiments, the initial pressure and temperature are set to 16 bar and 453 K, respectively. Note that the horizontal guide tube shown in Fig. 2 is also present in the experimental setup but not shown in Fig. 1.

CONVERGE CFD, release 3.0.16, is used to carry out the numerical simulations. CONVERGE is a general purpose computational fluid dynamics (CFD) solver that can handle compressible and incompressible reacting flows in complex three dimensional geometries. An orthogonal grid with a 1 mm base size is used in the computational domain. Several embedded refinements are included to achieve a minimum grid size of 62.5 μm at the spark plug gap, as shown in Fig. 2. The grid configuration and flow validation were assessed in previous work [17, 19]. First, the flow simulations without

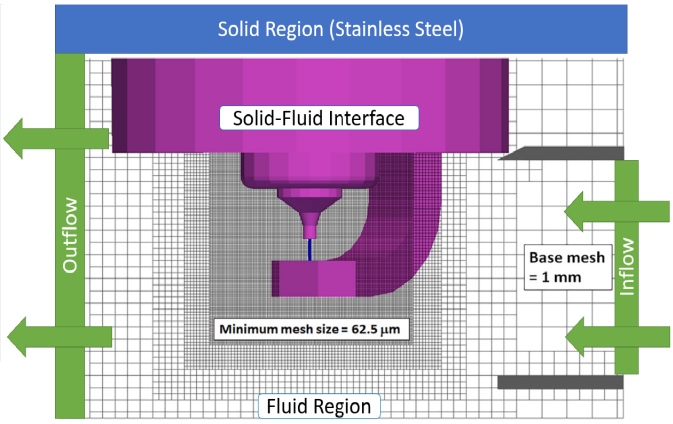

FIGURE 2. Simplified Computational Domain and Grid

the spark plug (replaced with adapter) were carried out until a pseudo-steady state was achieved and the velocity field was compared to PIV data. Then, the spark plug was added and the flow field was solved again to serve as an initial condition to ignition/combustion simulations.

The LESI model is used for ignition modeling. LESI is a line source spark ignition model developed to model the glow phase of ignition, in quiescent and cross-flow conditions using user defined functions (UDFs) within the CONVERGE CFD framework. LESI initializes the spark channel as series of connected particles, which are tracked in a Lagrangian fashion. The particles' movement is derived from the surrounding velocity field to account for spark channel impedance. The end particles of the spark channel are kept attached to the electrodes, while internal particles are allowed to move with the flow. As the spark channel increases in length, more internal particles are added to maintain adequate resolution of the spark channel (based on a predefined inter-particle distance). In addition, the model truncates the channel when an internal particle gets closer to the electrode surface than an end particle, therefore mimicking the behavior of electrical current. The source energy is divided equally between the Lagrangian particles and deposited as a volumetric source term in the Eulerian computational cells, where the particle exists at that instant in time. Further details and validation of LESI are available in [19]. The breakdown (or preglow) phase is evaluated offline using a two-step chemistry equilibrium scheme (Cantera) and the resulting temperature, pressure, and species composition are used as initial values for the glow phase modeled by LESI. For this experimental point, the breakdown phase is initialized as a cylinder with a 0.9 mm length (same as spark gap) and a diameter of 0.1 mm. The resulting temperature and pressure are 5000 K and 225 bar, respectively. The resulting species list is omitted here for brevity. Following the breakdown initialization, LESI deposits 30 mJ of energy during 1.7 ms, through its Eulerian energy deposition, and tracks the spark channel (start with 14 particles) and deposition sites using its Lagrangian approach, as discussed earlier. GRI-Mech 3.0 is adopted for combustion modeling and either re-normalization group (RNG) $k-\varepsilon$ within Reynolds-averaged Navier–Stokes (RANS) framework or Dynamic Structure within large-eddy simulation (LES) framework are used as turbulence models.

Arrhenius based well-stirred reactor (WSR), thickened-flame model (TFM) and flamelet based G-equation are used for combustion modeling. TFM relies on an artificial thickening scheme to resolve the flame front, which is located using a sensor function. Here, the sensor is based on heat release rate and not the more commonly used fuel species. Charlette's model [21] of the wrinkling factor is used to account for sub-grid scale (SGS) flame-turbulence interaction and reduced flame wrinkling brought by the artificial thickening. The G-equation model tracks the flame front by solving transport equations for G and G'' (G=0 at flame front). The Peters turbulent flame speed expression is used for RANS and the Pitsch expression is used for LES, as recommended by CONVERGE guidelines. For both TFM and G-equation, tabulated laminar flame speed values are used, which were generated offline using CONVERGE 1D laminar flame speed chemistry solver, for the pressure, temperature, equivalence ratio, and dilution levels present in the combustion vessel. The tabulated flame speed values were generated using the same chemical mechanism (GRI-Mech 3.0) used in TFM and WSR (detailed chemistry) models.

RESULTS

The results are split into two main parts. First, LESI is coupled with WSR (RANS and LES) and TFM (LES), to assess the robustness and consistency of spark channel elongation and flame progression as predicted by the model. Then, G-equation is used to locate the flame front, while WSR is still used in the burnt and unburnt regions. G-equation is the industry standard and most commonly used in automotive design. Results in both sections are compared to experimental Schlieren images.

ARRHENIUS COMBUSTION MODELS - WSR and TFM

Well-Stirred Reactor (WSR) In [19], LESI was validated in a RANS-WSR environment with a minimum grid size of 62.5 μm, which is the baseline case for this paper. In order to assess the robustness of the ignition model and the consistency of the results in different turbulence models and grid sizes, Fig. 4 shows results from experiment, the baseline case, a LES case with the same grid size as the baseline case, and a LES case with a minimum grid size of 31.25 μm. Note that when the grid sized is reduced by half, the number of initial LESI particles is doubled to maintain an average of one particle per computational cell. While this is a recommendation, it is not a requirement for

the LESI model. In fact using an average particles per cell larger than 1 is feasible and might at specific conditions yield better arc tracking. Also note that in the last row (time=2.0 ms), there are no Lagrangian particles because ignition has ended (at 1.7 ms). In Fig. 4, the experimental results are Schlieren images, while the simulation images are temperature contour plots (limited to temperatures higher than 500 K) with the LESI tracking particles in black. The flow field for all three simulation cases at start of ignition is shown in Fig. 3.

Figure 3 shows that LES generates a more time resolved flow field compared to RANS, which is time averaged. The bulk flow, however, especially at the spark gap, is comparable in velocity magnitude and location. Hence, the arc tracking in RANS and LES is expected to behave similarly. For a small controlled geometry, such as the case here, the difference in LES and RANS flow field is minimal, especially for fine grid sizes (62.5 μm and 31.25 μm). However, for an engine case, when such fine grids cannot be maintained for the entire engine geometry, and the flow field is highly dependent on the intake and exhaust strokes, the differences between LES and RANS are expected to be more pronounced and have a larger effect on ignition modeling. Here, for the purposes of showing the robustness and consistency of the results, similar flow fields between RANS and LES are desirable.

In Fig. 4 the results are consistent between the different turbulence models and grid sizes. While LESI particle motion is scaled by a user parameter (to mimic spark channel impedance) and could be allowed to elongate further, the arc tracking and flame growth are both well predicted. The shape of the arc in the last column (refined grid LES) is more rounded, which better matches the experiment, especially at later times. A higher grid resolution allows for a more accurate tracking of double the number of particles. While LESI derives its particle motion from the velocity field, a more time resolved field using LES did not produce significant differences compared to the time-averaged RANS, for this case. Perhaps for leaner cases with higher turbulence, or as mentioned earlier an engine simulation, the choice of turbulence model would affect arc tracking more significantly. Nevertheless, for this case, the arc location and flame growth are largely unaffected by the choice of turbulence model or further refinement beyond 62.5 μm. Since the grid is already at a similar size to the flame thickness for this case (50-100 μm), WSR model is sufficient for the early times of ignition, kernel formation, and flame growth. As the flame grows into the coarser regions of the grid, a turbulent flame propagation model is needed, as can be seen from the final two rows of Fig. 4 (time 1.5 and 2.0 ms), where the leading edge of the flame front does not propagate in the vertical direction to the extent observed in experimental images. On the other hand, the arc shape benefits from a finer grid (even smaller than the flame thickness) since the resolution of the arc is directly tied to the grid resolution (one LESI particle for every computational cell).

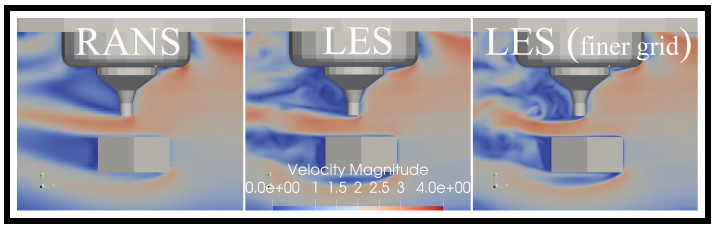

FIGURE 3. Center Plane Velocity Magnitude Baseline Cases. From Left to Right: RANS (Min. Grid Size 62.5 micron), LES (Min. Grid Size 62.5 micron), LES (Min. Grid Size 31.25 micron)

Thickened Flame Model (TFM) While a grid size of 62.5 μm may be suitable for accurate arc tracking and flame growth, the flame will eventually grow outside the refined fixed embedding into coarser regions with grid sizes of 125, 250, and even 500 μm (refer to Fig. 2). Given that 250-500 μm are typical grid sizes used in LES/RANS of engines, respectively, the WSR model would be incapable of resolving the flame front and accurately modeling flame growth. To remain within detailed chemistry models, TFM builds on top of WSR to resolve the flame front through manipulation of mixing and chemistry terms.

Since TFM alters the heat release properties of the flame, it is not recommended to be turned on along with energy deposition as it might affect the ignition behavior. Here TFM relies on a laminar flame speed table generated for propane, a flame sensor with Jaravel's adjustment, and Charlette's model for the wrinkling factor (sometimes called efficiency function), with an exponential power factor = 0.95. The flame speed table also contains flame thickness and reference reaction rates to be used in the flame sensor and efficiency function formulations. Ten grid points are utilized to cover the flame front, or in other words, the minimum grid size required to fully resolve the flame is 10% of the laminar flame thickness, as shown in Eq. 1.

$$F_{max} = \frac{n_{res}\Delta}{\delta_l^0} = \frac{\Delta}{\delta_l^0/n_{res}} \tag{1}$$

The maximum thickening factor F_{max} is the ratio of the grid size (or filter size Δ) to the minimum grid size required to fully resolve the flame (in this case assumed to be 10% of the flame thickness δ_l^0), which is equivalent of assuming n_{res}, the number of grid points across the flame, to be ten.

Figure 5 shows temperature contour plots, similar to the ones shown in Fig. 4, but the first plot is at 1.8 ms (not 0.1 ms) because TFM is turned on only after ignition is over at 1.7 ms. Assuming the high temperature region to be the burnt region, the effect of artificial thickening on flame propagation is observable from early on and increases with time. When compared to the Schlieren images, TFM improved the flame front in the vicinity of the spark gap (trailing edge) and at the

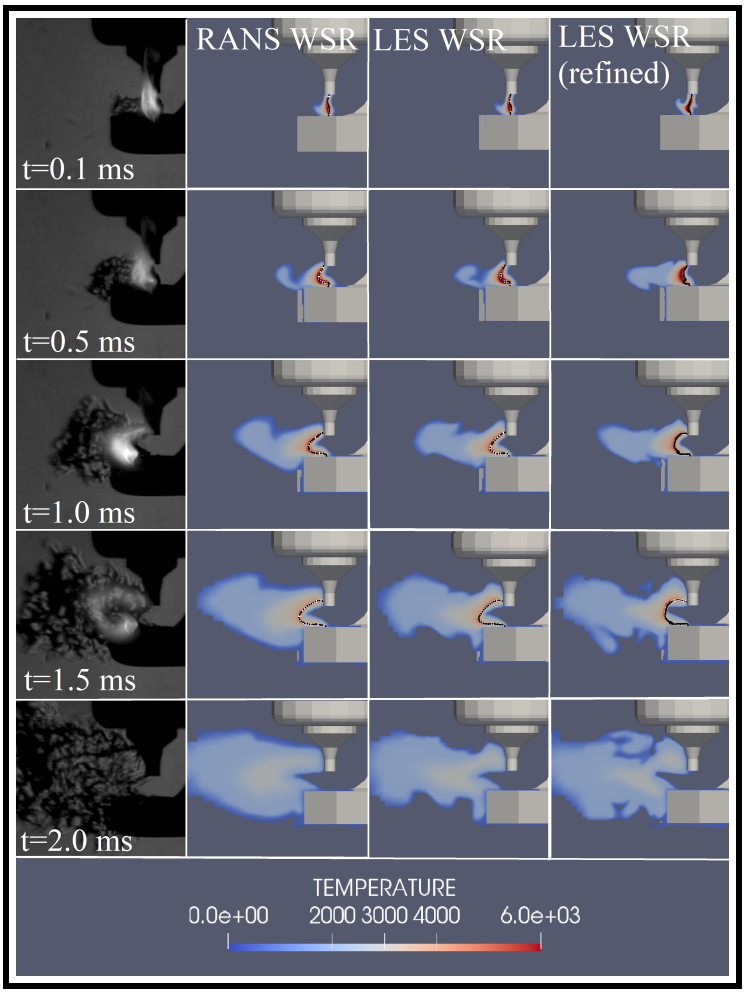

FIGURE 4. Center Plane Temperature Contour Plots and Arc Tracking using LESI for Baseline Cases. From Left to Right: Experimental Schlieren Images, RANS with WSR (Min. Grid Size 62.5 micron), LES with WSR (Min. Grid Size 62.5 micron), LES with WSR (Min. Grid Size 31.25 micron)

leading edge of the flame, as marked with red circles in Fig. 5. In this case, the improvement brought by TFM is not overly dramatic for two main reasons: first, the WSR model predicts a reasonable flame propagation rate, especially early on, due to a combination of fine grid resolution and stable conditions, and is not far off from experimental results. Second, TFM has been active for a short duration of time. By inspecting Fig. 4, the leading edge of the flame would benefit from TFM as early as 1 ms (as it starts to enter the coarser region of the grid). However, the accuracy of ignition and arc tracking would be jeopardized when thickening is applied to the trailing edge of the flame, where the Lagrangian particles are concentrated. While the coupling between LESI and WSR/TFM is seamless, due to the nature of energy deposition and Arrhenius terms, the switch

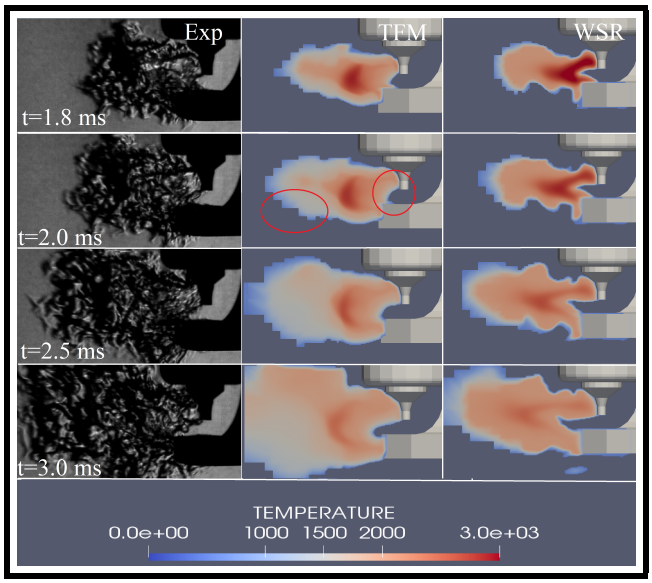

FIGURE 5. Center Plane Temperature Contour Plots using the Thickened Flame Model (TFM). From left to right: Experimental Schlieren Images, Thickened Flame Model (TFM), Well-Stirred Reactor (WSR)

between LESI/WSR to TFM is a critical aspect of ignition, and could benefit from a controlled artificial thickening scheme that is limited in scope, while ignition is active, and is planned for future work.

As time progresses, and the flame enters coarser regions of the grid, TFM becomes more important, as evident in Fig. 6, where the thickening factor F and efficiency function E are shown. The regions where F and E are larger than 1, are the flame front as recognized by the sensor. Figure 6 shows that the flame front is properly captured by model. In addition, the magnitude of F is significantly higher in the regions with coarser grids, as expected, and reaches values higher than 50 but is limited to values as low as 10-15 in the finer grid. Similarly, the efficiency function E follows the same trend as F, for two reasons. First, the artificial thickening reduces the flame fronts sensitivity to sub-grid wrinkling, which is compensated for through E. Second, with coarser grids, SGS turbulence is larger (less resolved velocity field), and its effect of flame wrinkling is also accounted for through E. Hence, TFM is working as intended and is critical for flame propagation in coarser grid sizes (typically larger than 100 μm, which are generally used for engine simulations).

In summary, the coupling between LESI and TFM/WSR is seamless and the combination of LESI/WSR at fine grids predicts arc tracking and early flame growth reasonably well. However, the transition from WSR to TFM, especially during ignition, is of great importance, as shown here. A hybrid approach of controlled and localized artificial thickening away from the

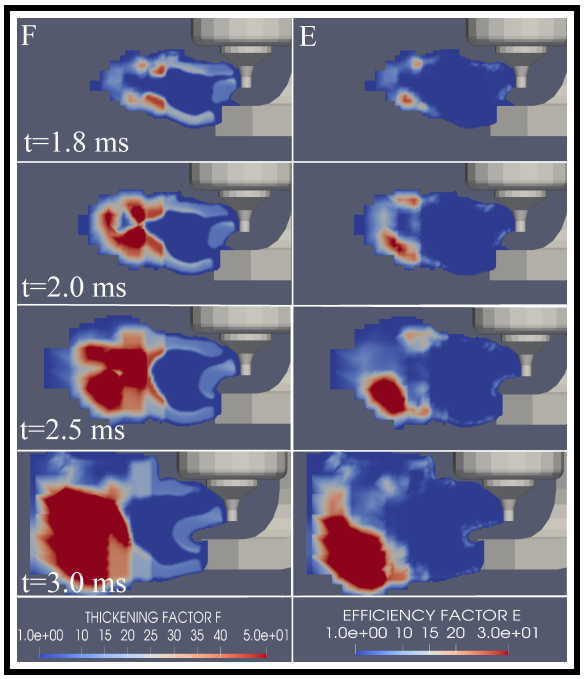

FIGURE 6. Center Plane Contour Plots using the Thickened Flame Model (TFM) for the Thickening Factor (F) and the Efficiency Function (E)

ignition region would be viable to reap the benefits of TFM at early stages of flame growth without affecting the arc tracking model.

FLAMELET COMBUSTION MODELS - G EQUATION

G-equation is perhaps the most used flame propagation model by automakers and coupling it with any ignition model is inherently of interest. G-equation relies on solving transport equations for G and G'', where G=0 is the defined as the flame front. G is controlled by different terms in its transport equation, but perhaps the most critical is the turbulent flame speed S_t. Within the RANS framework, S_t is based on the expression by Peters, which utilizes G'', while in the LES framework, S_t is based on the expression by Pitsch (For the full expressions refer to [18]).

In contrary to TFM, and since the variable G is artificial, the g-equation model is usually turned on from the start of ignition and plays a roles in the early flame formation and growth. In general, G-equation model relies on a g-sourcing scheme to initialize the flame front, which can be thought of as a very simplistic ignition model. As an alternative, energy deposition can be coupled with G which is initialized at temperatures higher than 3000 K using a temperature cut-off scheme, and allowed to propagate. Here, coupling LESI with G-equation is done in this manner.

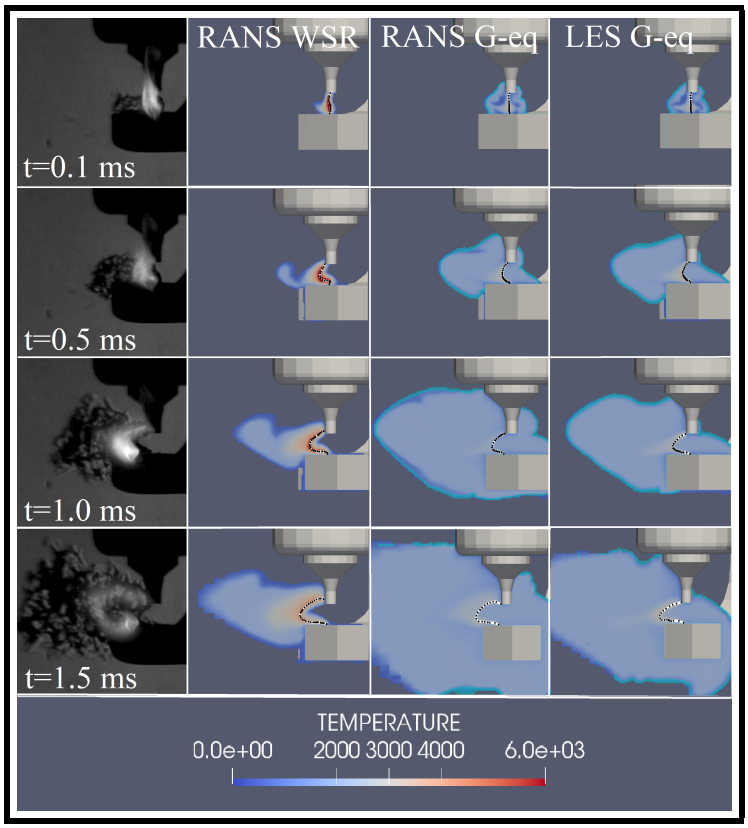

FIGURE 7. Center Plane Temperature Contour Plots and Arc Tracking using LESI and G-equation model. Shaded Edges denote Flame Front as Identified by G=0 Iso-surface. From left to right: Experimental Schlieren Images, RANS Well-Stirred Reactor (WSR, RANS G-Eq (Peters Correlation), LES G-Eq (Pitsch Correlation)

Figure 7 shows temperature contour plots, similar to the ones shown in Fig. 4. For the G-equation plots, the shaded area at the edge of the high temperature region is the flame front as identified by the G=0 iso-surface. Figure 7 shows that the G-equation model overestimates the flame growth, from early times, in both RANS and LES frameworks. On the other side, LESI is able to track the spark channel, despite the errors in flame propagation.

There are two possible reasons for the overestimation of flame growth by G-equation. First, the temperature cutoff scheme used to initialize G creates an initial flame front which is significantly far off from the real location. With time, the initial error amplifies and leads to larger inaccuracies. Figure 8 shows the flame front 1 μs after ignition, when G=0 is initialized, compared to the WSR case. It can be seen that while the initialization of G is not ideal, and could use improvement over the temperature cutoff method, the initial flame location is not far off from the real location.

The second possible reason is the flame propagation speed,

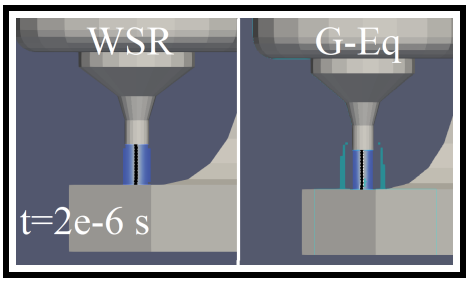

FIGURE 8. Center Plane Temperature Contour Plots using WSR and G-equation model at t=2 μs. Light Blue Edges denote Flame Front as Identified by G=0 Iso-surface.

which is mainly controlled by S_t. The G=0 iso-surface is allowed to propagate at S_l from its initiation. The early stages of flame kernel formation are controlled by the laminar flame speed S_l until the kernel reaches a large enough size to interact with turbulent eddies and wrinkle the flame front, after which it propagates at S_t. Hence, early flame development is overestimated and a laminar to turbulent transition scheme, as proposed in [5], is necessary.

On the other hand, coupling the G-eq model with the LESI (or any other energy deposition model) is feasible, by relying on the temperature cutoff approach. In fact, the Lagrangian arc tracking and Eulerien energy deposition work seamlessly with G-eq, using this approach. However, two important considerations, mainly concerned with flame growth, are:

1 - The initialization of the G=0 using temperature cutoff can be improved upon. A more involved formulation that relies on the energy deposition scheme and some other physical variable (such as heat release or flame surface density) might be more appropriate.

2 - The flame propagation speed at early stages of ignition cannot rely solely S_t, but a transition function between laminar and turbulent propagation is necessary, as suggested in [5].

Finally, quantitative comparison of the cases presented is appropriate here. Fig. 9 shows the flame propagation behavior between the different models compared to experiment. Fig. 9 was created directly by estimating the flame length and width from experiment and simulation results shown previously in this paper. The longitudinal flame propagation was measured from the center-line of the electrode, while the width of the flame was measured at its largest location. As expected, the G-eq model overestimates both metrics compared to experiment and the other models. The WSR model adequately predicts the flame length compared to experiment at early times but eventually under-predicts it at later times when the flame front reaches the coarser grid. On the other hand, it under-predicts the flame width at all times. TFM when turned on at 1.7 ms increases the flame

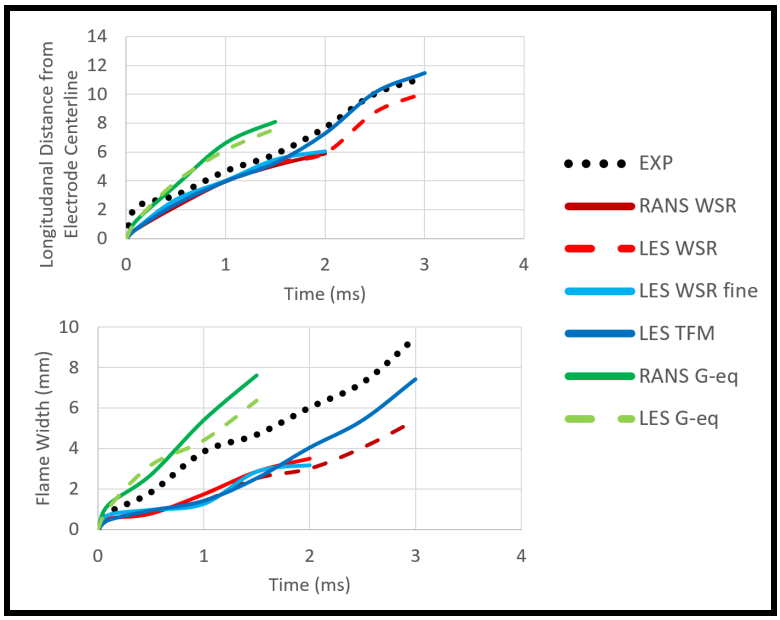

FIGURE 9. Flame Propagation Metrics for WSR, TFM, and G-eq models compared to Experiment

length to match experiment at later times. TFM also increases the flame width but not enough to match the experiment. The difference in model behavior highlights the need for G-eq model to better handle early flame formation and propagation and incorporate a laminar-to-turbulent transition, while WSR results can be improved by turning TFM on at an earlier time.

In addition, Fig. 10 shows the heat release rate (HRR) in the vessel for the different combustion models using LES and RANS turbulence models. Based on Fig. 9, the TFM HRR is expected to be closest to experimental HRR. As such, under-prediction in flame propagation (especially in flame width) by WSR at later times when the flame front reaches the coarser regions of the grid is reflected here on the HRR. Similarly the over-prediction of flame propagation by the G-eq model can also be seen in the HRR in Fig. 10. At 1 ms WSR HRR is around 0.24 J/ms and G-eq HRR is around 2 J/ms which is 8-9 times larger.

CONCLUSION

In this paper, a high-fidelity energy deposition ignition model was coupled with flame propagation models at engine-like flow conditions in a combustion vessel. The ignition model (LESI) combines Lagrangian arc tracking with Eulerian energy deposition to describe the glow phase of ignition.

First, LESI was coupled with the WSR in RANS and LES frameworks, at different grid resolutions. The coupling was seamless and relied on the temperature controlled Arrhenius detailed chemistry. The model showed robust and consistent results in all cases. At fine grid resolutions, the WSR is sufficient

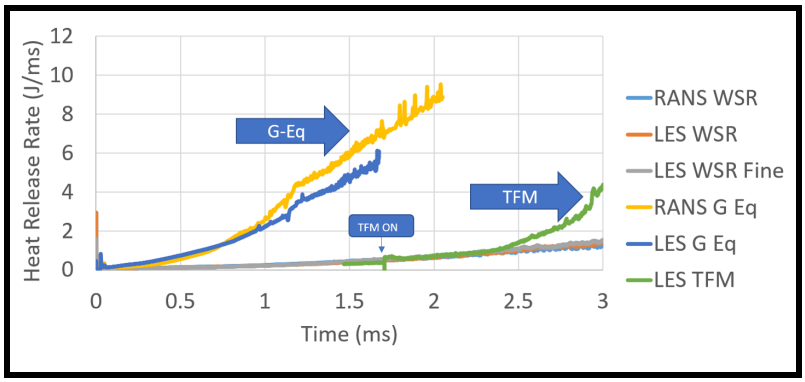

FIGURE 10. Heat Release Rate (HRR) in the combustion vessel for WSR, TFM, and G-eq models with LES and RANS Turbulence Models

to model early flame growth. The arc tracking, however, benefited (marginally) from refined grids and additional tracking particles.

Then, LESI was coupled with TFM, in a similar fashion as WSR, because both models are chemistry based. TFM was turned off during ignition to avoid affecting the spark channel tracking. Once TFM was turned on, it located the flame front and improved flame propagation accuracy. The transition from WSR to TFM was critical, and artificial thickening during ignition, especially on a coarse grid, should be considered, while not affecting the arc tracking accuracy.

Finally, LESI was coupled with the G-equation model through a temperature cutoff method. The model over-predicted the flame growth due to relying on S_t from the time of flame front initiation, while the spark channel elongation and arc tracking were unaffected. To improve the accuracy of flame growth, an improved initialization scheme is suggested. More importantly, expanding the G-Equation formulation during early flame kernel growth to account for laminar to turbulent transition is necessary.

In conclusion, LESI energy deposition can be coupled with flame propagation models and used to generate reasonable results in engines. While turbulent flame propagation is expected to be well predicted, more effort needs to be placed to develop transition functions from laminar kernel growth to full turbulent flames. Accurate ignition models are necessary to better predict cycle-to-cycle variability (CCV) in engines, especially in unconventional operation such as highly dilute.

NOMENCLATURE

AFCL Alternative Fuels Combustion Laboratory
AKTIM Arc and Kernel Tracking Ignition Model
CCV Cycle-to-Cycle Variability
CFD Computational Fluid Dynamics
δ_l^0 Laminar Flame Thickness
Δ Grid or Filter Size
DI Direct Injection
DPIK Discrete Particle Ignition Kernel
E Efficiency Function
ECFM Extended Coherent Flame Model
EGR Exhaust Gas Re-circulation
F Thickening Factor
F_{max} Maximum Thickening Factor
HRR Heat Release Rate
ISSIM Imposed Stretch Spark-Ignition Model
LDV Light Duty Vehicle
LES Large-Eddy Simulation
LESI Lagrangian-Eulerian Spark Ignition
MTU Michigan Technological University
n_{res} Number of Grid Points across the Flame Front
PFI Port Fuel Injection
PIV Particle Image Velocimetry
RANS Reynolds-Averaged Navier–Stokes
RNG Re-Normalization Group
SI Spark Ignition
SparkCIMM Spark Channel Ignition Monitoring Model
S_l Laminar Flame Speed
S_t Turbulent Flame Speed
TFM Thickened Flame Model
UDF User-defined function
WSR Well-Stirred Reactor

ACKNOWLEDGMENT

The submitted manuscript has been created by UChicago Argonne, LLC, Operator of Argonne National Laboratory ("Argonne"). Argonne, a U.S. Department of Energy Office of Science laboratory, is operated under Contract No. DE-AC02-06CH11357.

The U.S. Government retains for itself, and others acting on its behalf, a paid-up nonexclusive, irrevocable worldwide license in said article to reproduce, prepare derivative works, distribute copies to the public, and perform publicly and display publicly, by or on behalf of the Government.

This research is funded by DOE's Vehicle Technologies Program, Office of Energy Efficiency and Renewable Energy, under the FY19 Technology Commercialization Fund (TCF) program. The authors would like to express their gratitude to Gurpreet Singh and Mike Weismiller, program managers at DOE, for their support.

Numerical simulations were run on the Blues and Bebop Clusters at the LCRC, Argonne National Laboratory.

REFERENCES

[1] (EIA), U. S. E. I. A., 2021. *ANNUAL ENERGY OUTLOOK*.

[2] Ikeya, K., Takazawa, M., Yamada, T., Park, S., and Tagishi, R., 2015. "Thermal efficiency enhancement of a gasoline engine". *SAE International Journal of Engines,* ***8***(4), pp. 1579–1586.

[3] Ayala, F. A., and Heywood, J. B., 2007. "Lean si engines: The role of combustion variability in defining lean limits". In SAE Technical Paper, Consiglio Nazionale delle Ricerche.

[4] Colin, O., and Truffin, K., 2011. "A spark ignition model for large eddy simulation based on an fsd transport equation (issim-les)". *Proceedings of the Combustion Institute,* ***33***(2), pp. 3097–3104.

[5] Keum, S., Zhu, G., Ronald Grover, J., Zeng, W., Rutland, C., and Kuo, T.-W., 2021. "A semi-empirical laminar-to-turbulent flame transition model coupled with g equation for early flame kernel development and combustion in spark-ignition engines". *International Journal of Engine Research,* ***22***(2), pp. 479–490.

[6] Thiele, M., Selle, S., Riedel, U., Warnatz, J., and Maas, U., 2000. "Numerical simulation of spark ignition including ionization". *Proceedings of the Combustion Institute,* ***28***(1), pp. 1177–1185.

[7] Yang, X., Solomon, A., and Kuo, T.-W., 2012. "Ignition and combustion simulations of spray-guided sidi engine using arrhenius combustion with spark-energy deposition model". In SAE 2012 World Congress & Exhibition, SAE International.

[8] Givler, S. D., Raju, M., Pomraning, E., Senecal, P. K., Salman, N., and Reese, R., 2013. "Gasoline combustion modeling of direct and port-fuel injected engines using a reduced chemical mechanism". In SAE Technical Paper, SAE International.

[9] Tan, Z., and Reitz, R. D., 2006. "An ignition and combustion model based on the level-set method for spark ignition engine multidimensional modeling". *Combustion and Flame,* ***145***(1), pp. 1–15.

[10] Duclos, J.-M., and Colin, O., 2001. "(2-25) arc and kernel tracking ignition model for 3d spark-ignition engine calculations((si-7)s. i. engine combustion 7-modeling)". *The Proceedings of the International symposium on diagnostics and modeling of combustion in internal combustion engines,* ***01.204***, p. 46.

[11] Dahms, R. N., Drake, M. C., Fansler, T. D., Kuo, T.-W., and Peters, N., 2011. "Understanding ignition processes in spray-guided gasoline engines using high-speed imaging and the extended spark-ignition model sparkcimm. part a: Spark channel processes and the turbulent flame front propagation". *Combustion and Flame,* ***158***(11), pp. 2229–2244.

[12] Dahms, R., Fansler, T., Drake, M., Kuo, T.-W., Lippert, A., and Peters, N., 2009. "Modeling ignition phenomena in spray-guided spark-ignited engines". *Proceedings of the Combustion Institute,* ***32***(2), pp. 2743–2750.

[13] Fan, L., Li, G., Han, Z., and Reitz, R. D., 1999. "Modeling fuel preparation and stratified combustion in a gasoline direct injection engine". In International Congress & Exposition, SAE International.

[14] Sayama, S., Kinoshita, M., Mandokoro, Y., Masuda, R., and Fuyuto, T., 2018. "Quantitative optical analysis and modelling of short circuits and blow-outs of spark channels under high-velocity flow conditions". In SAE Technical Paper, SAE International.

[15] Masuda, R., Sayama, S., Fuyuto, T., Nagaoka, M., Sugiura, A., and Noguchi, Y., 2018. "Application of models of short circuits and blow-outs of spark channels under high-velocity flow conditions to spark ignition simulation". In SAE Technical Paper, SAE International.

[16] Ge, H., and Zhao, P., 2018. "A comprehensive ignition system model for spark ignition engines". *Volume 2: Emissions Control Systems; Instrumentation, Controls, and Hybrids; Numerical Simulation; Engine Design and Mechanical Development*.

[17] Zhang, A., Scarcelli, R., Lee, S.-Y., Wallner, T., and Naber, J., 2016. "Numerical investigation of spark ignition events in lean and dilute methane/air mixtures using a detailed energy deposition model". In SAE Technical Paper, SAE International.

[18] Richards, K. J., Senecal, P. K., and Pomraning, E., 2021. *CONVERGE 3.0*. CONVERGENT SCIENCE, Madison, WI.

[19] Scarcelli, R., Zhang, A., Wallner, T., Som, S., Huang, J., Wijeyakulasuriya, S., Mao, Y., Zhu, X., and Lee, S.-Y., 2019. "Development of a hybrid lagrangian-eulerian model to describe spark-ignition processes at engine-like turbulent flow conditions". *Journal of Engineering for Gas Turbines and Power,* ***141***(9).

[20] Zhu, X., Sforza, L., Ranadive, T., Zhang, A., Lee, S.-Y., Naber, J., Lucchini, T., Onorati, A., Anbarasu, M., and Zeng, Y., 2016. "Experimental and numerical study of flame kernel formation processes of propane-air mixture in a pressurized combustion vessel". *SAE International Journal of Engines,* ***9***(3), pp. 1494–1511.

[21] Charlette, F., Meneveau, C., and Veynante, D., 2002. "A power-law flame wrinkling model for les of premixed turbulent combustion part i: non-dynamic formulation and initial tests". *Combustion and Flame,* ***131***(1), pp. 159–180.